Acc. Chem. Res. **1998,** *31,* 511−518

Conical Intersections: Diabolical and Often Misunderstood

DAVID R. YARKONY

Department of Chemistry, Johns Hopkins University, Baltimore, Maryland 21218

Received November 14, 1997

I. Introduction

Within the Born−Oppenheimer approximation nuclei move on the single potential energy surface created by the faster moving electrons. This approximation is the basis of our understanding of chemical bonding and molecular dynamics. Despite its central position in chemical theory breakdowns of the Born−Oppenheimer approximation, electronically nonadiabatic processes are ubiquitous. Nonadiabatic processes include charge transfer,[1] electronic quenching, and spin-forbidden[2] reactions. Many photochemical reactions are nonadiabatic,[3] including some of nature's most basic processes, the initial radiationless energy transport step in photosynthesis[4] and the cis−trans isomerization that initiates the process of vision.

In a nonadiabatic process the nuclei move on more than one Born−Oppenheimer potential energy surface. Nonadiabatic transitions result when the nuclei encounter a region where two potential energy surfaces are in close proximity. Regions where the potential energy surfaces intersect are of preeminent importance.

The nuclear coordinate dependence of the potential energy surfaces near the intersection is key to understanding the effect of the intersection on nuclear motion. While an infinite variety of intersections are possible, it is usual to distinquish the two types of intersections depicted in Figure 1. For the Renner−Teller or glancing intersection, Figure 1a, the potential energy surfaces depend quadratically on the nuclear coordinates near the crossing. In Figure 1b, the potential energy surfaces depend linearly on the nuclear coordinates and the confluence is referred to as a conical intersection since the local topology is that of a double cone. Berry has noted that this conical topology resembles that of a diabolo and has referred to points of conical intersection as diabolical points.[5]

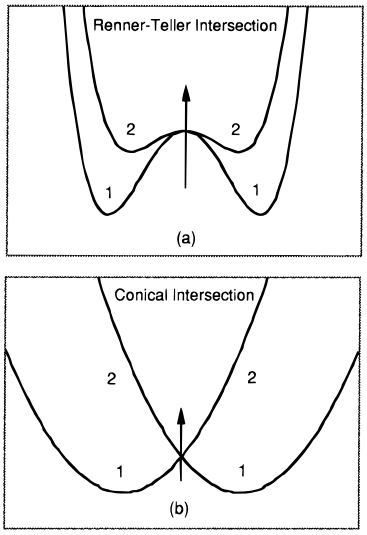

FIGURE 1. Section of (a) Renner−Teller intersection and (b) a general conical intersection. Potential energy surfaces are surfaces of revolution about indicated axis.

Conical intersections are the subject of this account. Intersections of potential energy surfaces were reviewed previously in this venue almost a quarter century ago.[6] This account explains how recent work has led to a rethinking of what was then the conventional wisdom about conical intersections. The conical topology is responsible for the important effects induced by this class of intersection. In the excited state the molecule is funneled into the region of the conical intersection, facilitating radiationless decay. On the ground-state potential energy surface a conical intersection produces the geometric phase (sometimes referred to as the Berry phase[7]) effect.[8−10] This signature property of a conical intersection requires that the adiabatic electronic wave function changes sign when transported along a closed loop—a pseudorotation path—surrounding (only) that point of conical intersection. However, not all pseudorotation paths surrounding a conical intersection are equivalent. A particular plane containing the conical intersection point, referred to here as the $g-h$ plane, is privileged. This plane and its use in analyzing conical intersections provide unifying themes for this work.

Of particular interest will be the locus of points of conical intersection and the role—or more precisely the lack of a role—played by point group symmetry in determining this locus. It will be shown that intersections allowed by symmetry need not be the whole story in a particular region of nuclear coordinate space. Additional conical intersections may exist in the *same* region. This occurrence has important implications for nonadiabatic nuclear dynamics and can be anticipated using recently developed computational tools.[11]

Another key to understanding a nonadiabatic process is the derivative coupling,

$$f^{IJ}_{\tau}(\mathbf{R}) \equiv \left\langle \Psi_I(\mathbf{r};\mathbf{R}) \middle| \frac{\partial}{\partial \tau} \Psi_J(\mathbf{r};\mathbf{R}) \right\rangle_{\mathbf{r}}$$

David R. Yarkony was born in New York, NY, in 1949. He received his bachelor's degree from the State University of New York at Stony Brook in 1971 and his Ph.D. with Henry F. Schaefer III at the University of California at Berkeley in 1975 and was a postdoctoral research associate of Robert J. Silbey at the Massachusetts Institute of Technology from 1976 to 1977. He joined the chemistry faculty at Johns Hopkins University in 1977 where he is now Professor of Chemistry. His prinicipal research interest is the theoretical treatment of electronically nonadiabatic processes.

S0001-4842(97)00113-1 CCC: $15.00
Published on Web 05/20/1998

where **r** and **R** denote the electronic and nuclear coordinates, τ is an internal nuclear coordinate, and $\Psi_I(\mathbf{r};\mathbf{R})$ is an adiabatic electronic state. This interaction, which induces nonadiabatic transitions between adiabatic states I and J, has traditionally been thought of as difficult to evaluate, although this is not the case.[12] In the absence of the derivative coupling, conical intersections would be of limited importance as funnels, since, as discussed below, they occupy negligible volume in nuclear coordinate space. The derivative coupling "expands" the effective region of action of conical intersections to a finite volume in nuclear coordinate space, enabling them to exert significant influence on nuclear dynamics. However, as a consequence of the geometric phase effect, the derivative coupling is singular at a conical intersection. To remove this singularity it is common to transform the adiabatic states to diabatic states, $\Psi_I^d(\mathbf{r};\mathbf{R})$. The construction of diabatic states from adiabatic states has long been a problem of considerable interest and controversy since "rigorous" diabatic states, that is, states for which

$$f_\tau^{d,IJ}(\mathbf{R}) \equiv \left\langle \Psi_I^d(\mathbf{r};\mathbf{R}) \middle| \frac{\partial}{\partial \tau} \Psi_J^d(\mathbf{r};\mathbf{R}) \right\rangle_\tau = 0 \quad [13]$$

do not exist for triatomic or larger molecules.[14] In this account a transformation to approximate diabatic states removing the perponderance of the derivative coupling near a conical intersection, and certainly all the singularity, is discussed.

Section II reviews the basic ideas about conical intersections and presents new findings from our recent research using a practical example[15] and a simple mathematical model to guide the discussion. Section III refines the discussion of section II considering current computational issues associated with conical intersections. The results presented in sections II and III could not have been obtained without recently developed algorithms[16] (see also ref 17) that locate conical intersections directly, that is, without prior determination of the potential energy surfaces themselves. Section IV summarizes and suggests directions for future investigations.

II. Conical Intersections

Conventional Wisdom and Conventional Misconceptions. (a) Classification of Conical Intersections: Role of Point Group Symmetry. Conical intersections are usually classified according to the role played by point group symmetry in their existence. Intersections are *symmetry-required* when the two electronic states form the components of a degenerate irreducible representation as in the Jahn−Teller intersection of the two lowest electronic states in Na_3 which correspond to the components of an E type irreducible representation of the point group C_{3v}.

The two remaining classes of conical intersections are *accidental* intersections. *Symmetry-allowed* accidental intersections correspond to the intersection of two states of distinct spatial symmetry. The two lowest excited singlet electronic states of H−S−H, the $1^1A''$ and $2^1A''$ states, provide an example of this type of conical intersection. For C_s geometries these states have the same symmetry and (are conventionally thought to) yield only avoided intersections.[18] For C_{2v} geometries these states are of $^1A_2$ and $^1B_1$ symmetry, so that symmetry-allowed accidental conical intersections may, and in fact do, occur.[19,18]

This conventional interpretation,[20,6] in which an intersection of potential energy surfaces originates as a consequence of point group symmetry and states of the same symmetry avoid one another, is widely held. These notions follow from the noncrossing rule for diatomic molecules (see refs 21 and 22 and below) according to which only states of distinct symmetry can cross (except in the rarest of circumstances). However, it has been emphasized[23] that in triatomic or larger molecules the noncrossing rule permits states of the same symmetry to intersect.[24] We will refer to such accidental intersections as *same-symmetry* conical intersections. The existence of same-symmetry intersections was a matter of some controversy 2 decades ago.[25] However recent computational advances[17,16] have made their determination relatively straightforward and have shown that they are not at all uncommon, opening new avenues of investigation.[10] An example of such an intersection is provided by the excited $1^1A''$ and $2^1A''$ states of the methyl analogue of H−S−H, methyl mercaptan, CH_3−S−H. This molecule clearly cannot have the C_{2v} structures that yield the symmetry-allowed accidental intersections in H−S−H, but does in fact exhibit conical intersections.[26]

(b) Simple Model for a Conical Intersection. The above classifications can be understood from the following real-valued 2 × 2 Hamiltonian matrix:

$$\boldsymbol{H}(\mathbf{R}) = \begin{pmatrix} S(\mathbf{R}) + G(\mathbf{R}) & V(\mathbf{R}) \\ V(\mathbf{R}) & S(\mathbf{R}) - G(\mathbf{R}) \end{pmatrix} \quad (1)$$

which has eigenvalues

$$E_\pm(\mathbf{R}) = S(\mathbf{R}) \pm [G(\mathbf{R})^2 + V(\mathbf{R})^2]^{1/2} \quad (2)$$

and will have degenerate eigenvalues (confluences) for $\mathbf{R} = \mathbf{R}_x$ such that

$$G(\mathbf{R}_x) = 0 \quad (3a)$$

$$V(\mathbf{R}_x) = 0 \quad (3b)$$

Here and below a general point of conical intersection is denoted $\mathbf{R}_x$. The **R**-dependence of G and V near $\mathbf{R}_x$ is the same for the symmetry-required, symmetry-allowed, and same-symmetry conical intersections, so that topologically speaking they are equivalent. The distinctions arise from the role played by group theory in finding solutions of eqs 3a and 3b.

(i) For *symmetry-required intersections* solutions of both (3a) and (3b) are determined by symmetry, that is, those **R** for which the molecule has the correct symmetry provide solutions of both (3a) and (3b). D_{3h} geometries, for example, result in an E state degeneracy in Na_3. Such geometries are easy to spot.

(ii) For *symmetry-allowed intersections* $V(\mathbf{R}_x) = 0$ by symmetry but $G(\mathbf{R}_x) = 0$ by happenstance; that is, not all $\mathbf{R}$ with the appropriate symmetry to satisfy (3b) must satisfy (3a). On the other hand the range of $\mathbf{R}$ is restricted to those geometries that give the molecule the point group symmetry in question. In the H_2S example cited above, restriction to C_{2v} geometries guarantees that $V(\mathbf{R}_x) = 0$. However, not all C_{2v} geometries give rise to conical intersections.

(iii) For *same-symmetry intersections* point group symmetry is of no help since both (3a) and (3b) are satisfied by happenstance. These intersections are difficult to anticipate.

The above classifications need not be topologically isolated in the sense that accidental (see below) or symmetry-required (see ref 27) degeneracies may be embedded in same-symmetry manifolds.

c. Practical Example: Al(^{2}P) + H_2. An example of considerable practical importance,[15] the reaction of ground-state Al(^{2}P) with H_2 on the $1^2A'$ and $2^2A'$ potential energy surfaces of the supermolecule AlH_2

$$Al(^2P) + H_2 \rightarrow AlH_2(1^2A_1, 1^2B_2) \rightarrow AlH_2(X^2A_1) \quad (4)$$

will be used as illustration. For C_{2v} structures the $1^2A'$ and $2^2A'$ states have $^2A_1$ and $^2B_2$ symmetry. Reaction 4 is relevant to the use of Al doped cryogenic hydrogen as an energetic material since formation of the dihydride AlH_2-(X^2A_1) could limit the stability of the van der Waals complex Al$-H_2$ that constitutes the energetic material.

(d) Locus of Points of Conical Intersection. Conical intersections are not isolated points but rather are continuously connected, forming a line, or generalized line, of dimension $N^{int} - 2$, where N^{int} is the number of internal degrees of freedom. The $N^{int} - 2$-dimensionality of the line (or seam) of conical intersection is easily rationalized from eqs 3a and 3b. Each of (3a) and (3b) is satisfied on a surface of dimension $N^{int} - 1$. The intersection of two surfaces of dimension $N^{int} - 1$ is a line of dimension $N^{int} - 2$. The noncrossing rule does not guarantee that potential energy surfaces will intersect, only that such intersections are possible.

(i) Conical Intersections and Transition States. For Al(^{2}P) + H_2, a $^2B_2-^2A_1$ symmetry-allowed line of conical intersection, $\mathbf{R}_x(r)$, must be described where r is the H$-$H distance. The situation is summarized in Figure 2, where the line of conical intersection is seen to "separate" the $^2B_2$ van der Waals minimum from the $^2A_1$ dihydride minimum. Walking along the seam of conical intersection, by incrementing r, the lower potential energy surface looks like a ridge. The minimum energy point on the seam, $\mathbf{R}_{MECP}$, is the $\mathbf{R}_x(r)$ for which $E_{1^2A'}(\mathbf{R}_x(r))$ is minimized. Near $\mathbf{R}_{MECP}$ is the mountain pass (not shown in Figure 2) that represents the true transition state, $\mathbf{R}_{TS}$, separating the van der Waals and dihydride minima. $\mathbf{R}_{TS}$ occurs at a C_s geometry. For such C_s geometries near a seam only avoided intersections are expected. The proximity of $\mathbf{R}_{TS}$ and $\mathbf{R}_{MECP}$ can lead to a nonadiabatic phenomenon, nonadiabatic recrossing.[28] In nonadiabatic recrossing

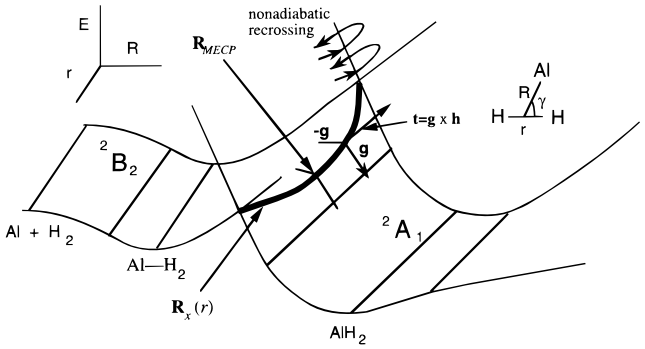

FIGURE 2. C_{2v} section of the $1^2A'$ and $2^2A'$ potential energy surfaces of AlH_2 and the Jacobi coordinates r, R, γ and the vector $\nabla G(\mathbf{R}) = \mathbf{g}$. The direction $\nabla V(\mathbf{R}) = \mathbf{h}$ for which a similiar ridge exists is not shown.

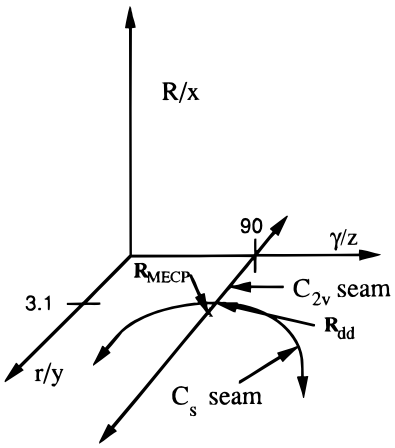

FIGURE 3. Schematic representation of the seam of conical intersection in AlH_2. R-dependence suppressed for clarity. The x, y, z labels refer to the example in section IIe (with a redefinition of the z-axis).

nuclear motion cannot follow the adiabatic *reactive* pathway owing to derivative couplings. Instead a *nonreactive*, nonadiabatic pathway is followed so that the region is repeatedly "recrossed". Nonadiabatic recrossing at a seam of conical intersection is illustrated in Figure 2.

(ii) Confluences of Confluences. In the above discussion we have used the conventional notion that the seam of conical intersection is an isolated feature so that away from the seam only avoided intersections are found. It turns out that this conventional wisdom fails dramatically for AlH_2. Figure 3 presents, for AlH_2, a schematic represention of the locus of points on the $1^2A'-2^2A'$ seam of conical intersection using the Jacobi coordinates given in Figure 2, mathematically $\mathbf{R}_x(r) = (R(r), r, \gamma(r))$ for which $E_{1^2A'}(\mathbf{R}_x(r)) = E_{2^2A'}(\mathbf{R}_x(r))$.[15] Conventionally it would be expected that $\gamma(r) = 90°$ for all r. However, this is plainly not the case! For $r < \sim 3.1a_0$, $\gamma(r) = 90°$. However for each $r > \sim 3.1a_0$ there are *three* points of conical intersection. One has $\gamma = 90°$ and is part of the C_{2v} seam. There are also two equivalent points with $\gamma = \gamma_x$, $180° - \gamma_x$ having only C_s symmetry. It is important to emphasize that all $\mathbf{R}_x$ are on the $1^2A'-2^2A'$ seam of conical intersection. This unusual feature represents a trifurcation of the C_{2v} seam as r increases past $\sim 3.1a_0$. Equivalently it is the

intersection of a C_s seam and a C_{2v} seam at the C_{2v} point $\mathbf{R}_{dd}$.

The importance of this feature cannot be overemphasized. Its existence means that the significant nonadiabatic effects associated with conical intersections cannot automatically be assumed to exist *only* for nuclear configurations yielding symmetry-allowed intersections. Additional confluences are possible in *unexpected* regions of nuclear coordinate space and may result in "confluences of confluences". Since points of conical intersection are referred to as diabolical points, the points at the intersection of two seams of conical intersection are referred to as doubly diabolical points.[11] The fact that this feature resembles the Mephistophelian trident (see Figure 3) is emblematic of its diabolical nature. The three-pronged pitchfork configuration is consistent with the continuity of the geometric phase effect as the trifurcation is encountered, whereas a two-pronged pitchfork, where the C_{2v} branch terminates at the intersection with the C_s branch, a bifurcation, is not.[15]

While it may be thought that doubly diabolical points are rare, such may not be the case. Doubly diabolical points have been found for the $1,2^1A'$ states of O_3,[29] the $2,3^3A''$ states of CH_2,[18] and the $1,2^2A'$ states of BH_2.[30] An important avenue for future investigation will be to understand the circumstances under which doubly diabolical points exist in triatomic and more general polyatomic molecules.

The dynamics in the region of doubly diabolical points is expected to be particularly interesting. The case of AlH_2 is quite compelling since, as Figure 3 indicates, $\mathbf{R}_{dd}$ occurs near $\mathbf{R}_{MECP}$ and hence near $\mathbf{R}_{TS}$. This region of nuclear coordinate space may well effect the predissociation rate of excited vibrational resonances of the dihydride AlH_2-(X^2A_1).[15]

(e) Tangent to the Seam of Conical Intersection. The tangent to the line of conical intersection, $\mathbf{t}(\mathbf{R}_x)$ (Figure 2), provides valuable information concerning the conical intersection and can be used to establish the existence of a doubly diabolical point. In the model problem the normal to the surface $G(\mathbf{R}) = 0$ is $\nabla G(\mathbf{R}) \equiv \mathbf{g}(\mathbf{R})$ and the normal to $V(\mathbf{R}) = 0$ is $\nabla V(\mathbf{R}) \equiv \mathbf{h}(\mathbf{R})$. Thus, at each $\mathbf{R}_x$, the degeneracy is lifted in a *linear* manner along the directions $\mathbf{g}(\mathbf{R}_x)$ and $\mathbf{h}(\mathbf{R}_x)$. The cross product, $\mathbf{g}(\mathbf{R}_x) \times \mathbf{h}(\mathbf{R}_x)$, therefore gives (for $N^{int} = 3$) $\mathbf{t}(\mathbf{R}_x)$. See Figure 2. A simple illustration is useful. See Figure 4. Let $G(x,y,z) = x$ and $V(x,y,z) = z$ so that the seam of conical intersection $G(x,y,z) = V(x,y,z) = 0$ is the y-axis, the set of all points with $x = z = 0$. But $\nabla G(\mathbf{R}) = \hat{\imath}$ and $\nabla V(\mathbf{R}) = \hat{k}$, so that $\hat{\imath} \times \hat{k} = -\hat{\jmath}$ as required.

The Hamiltonian with

$$G(\mathbf{R}) = x \qquad V_1(\mathbf{R}) = z \qquad V_2(\mathbf{R}) = y - a - z^2$$
$$V = V_1 V_2 \quad (5)$$

exhibits two intersecting seams of conical intersection analogous to those in AlH_2; see Figure 3: seam1 (the analogue of the C_{2v} seam) $\mathbf{R}_x(y) = (x = 0, y, z = 0)$, the y-axis, for which $G(\mathbf{R}_x) = V_1(\mathbf{R}_x) = 0$, and seam2 (the

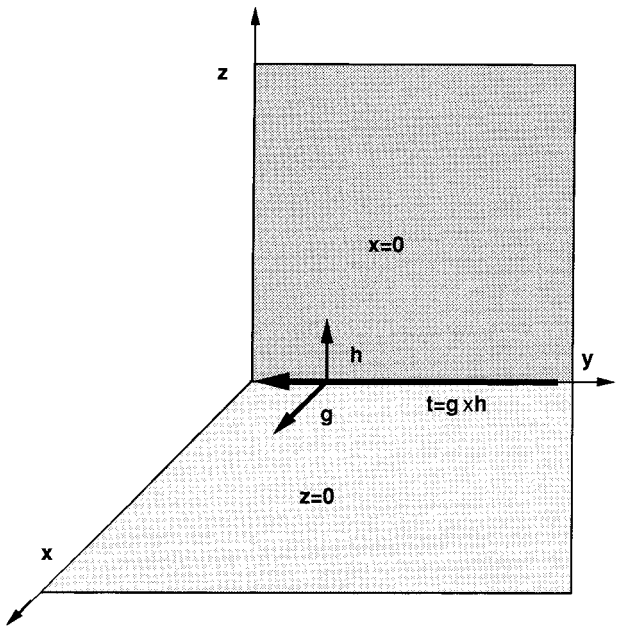

FIGURE 4. Surfaces $G(\mathbf{R}) = x = 0$, $V(\mathbf{R}) = z = 0$, the surface normals $\nabla G(\mathbf{R}) = \hat{\imath}$, $\nabla V(\mathbf{R}) = \hat{\jmath}$, and cross-product $\mathbf{t} = \hat{k}$.

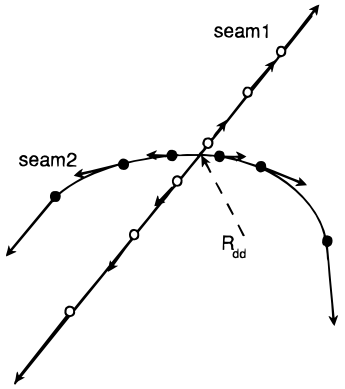

FIGURE 5. $\mathbf{t}$ along seam1 (C_{2v} seam) and seam2 (C_s seam) of Figure 3. $|\mathbf{t}|$ proportional to length of arrow.

analogue of the C_s seam) $\mathbf{R}_x(z) = (x = 0, y = a + z^2, z)$ for which $G(\mathbf{R}_x) = V_2(\mathbf{R}_x) = 0$. $\mathbf{R}_{dd} = (0, a, 0)$ is a doubly diabolical point. $\mathbf{t}(\mathbf{R}_x)$ for $\mathbf{R}_x$ on seam1 is $\mathbf{t}(y) = (a - y)\hat{\jmath}$ and on seam2 is $\mathbf{t}(z) = z(2z\hat{\jmath} + \hat{k})$. Note that near $\mathbf{R}_{dd}$ $\mathbf{t}(w)$ is an odd function of w to lowest order, so that $\mathbf{t}$ changes sign while passing through $\mathbf{R}_{dd}$ where it vanishes. This behavior, which is illustrated in Figure 5, can be used to efficiently locate doubly diabolical points (see below and refs 11 and 30). Since $\mathbf{t}$ vanishes at $\mathbf{R}_{dd}$, $\mathbf{g}(\mathbf{R}_{dd})$ and $\mathbf{h}(\mathbf{R}_{dd})$ are not linearly independent there and the local topology is not that of a double cone. $\mathbf{R}_{dd}$ is however the limit of two sequences of points with the double cone topology.

III. More Detailed Analysis

The foundation of this section is a perturbative analysis of the wave functions near a conical intersection[32] which is a generalization of the degenerate perturbation theory introduced by Mead[31] to treat conical intersections in X_3 systems, a work of fundamental importance. This analysis (i) leads to an algorithm that locates conical intersections

directly, that is, without prior determination of the potential energy surfaces themselves, (ii) permits the existence of doubly diabolical points to be anticipated,[11] and (iii) defines a locally diabatic basis, that is, $\Psi_I^d(\mathbf{r};\mathbf{R})$ for which $\mathbf{f}^{d,IJ}(\mathbf{R}) \sim \mathbf{0}$, for $\mathbf{R}$ near $\mathbf{R}_x$.

In X_3 molecules the *plane* containing the pseudorotation paths that give rise to the geometric phase effect is determined by symmetry. For general polyatomic molecules this is not the case. The perturbative analysis clarifies the nature of this plane in general polyatomic molecules.

(a) The g−h Plane and Pseudorotation. The adiabatic wave functions $\Psi_I(\mathbf{r};\mathbf{R})$, are expanded in a basis of symmetry-adapted Slater determinants $\psi(\mathbf{r};\mathbf{R})$

$$\Psi_I(\mathbf{r};\mathbf{R}) = \sum_{\alpha=1}^{N^{CSF}} c_\alpha^I(\mathbf{R})\, \psi_\alpha(\mathbf{r};\mathbf{R}) \tag{6}$$

where the $\mathbf{c}^I(\mathbf{R})$ satisfy the configuration interaction problem:

$$[\boldsymbol{H}(\mathbf{R}) - E_I(\mathbf{R})]c^I(\mathbf{R}) = 0 \tag{7}$$

We are concerned with $\mathbf{R} = \mathbf{R}_x$ for which $E_I(\mathbf{R}) = E_J(\mathbf{R})$ with $J = I + 1$. The key quantities are

$$g_\tau^L(\mathbf{R}) = \mathbf{c}^L(\mathbf{R}_x)^\dagger \frac{\partial \boldsymbol{H}(\mathbf{R})}{\partial \tau} \mathbf{c}^L(\mathbf{R}_x) \qquad L = I,J \tag{8a}$$

$$h_\tau^{IJ}(\mathbf{R}) = \mathbf{c}^I(\mathbf{R}_x)^\dagger \frac{\partial \boldsymbol{H}(\mathbf{R})}{\partial \tau} \mathbf{c}^J(\mathbf{R}_x) \tag{8b}$$

$$2g_\tau^{IJ}(\mathbf{R}) \equiv g_\tau^I(\mathbf{R}) - g_\tau^J(\mathbf{R}) = [\mathbf{c}^I(\mathbf{R}_x) + \mathbf{c}^J(\mathbf{R}_x)]^\dagger \frac{\partial \boldsymbol{H}(\mathbf{R})}{\partial \tau} [\mathbf{c}^I(\mathbf{R}_x) - \mathbf{c}^J(\mathbf{R}_x)] \tag{8c}$$

$\mathbf{g}^{IJ}(\mathbf{R}_x)$ and $\mathbf{h}^{IJ}(\mathbf{R}_x)$, the analogues of $\mathbf{g}$ and $\mathbf{h}$ defined in section II, are the generalizations for an arbitrary conical intersection of the E_x and E_y modes in the classic X_3 Jahn−Teller problem. $\mathbf{g}^{IJ}(\mathbf{R}_x)$ and $\mathbf{h}^{IJ}(\mathbf{R}_x)$ define the $g-h(\mathbf{R}_x)$ plane, and $\mathbf{t}^{IJ}(\mathbf{R}_x) \equiv \mathbf{g}^{IJ}(\mathbf{R}_x) \times \mathbf{h}^{IJ}(\mathbf{R}_x)$, the direction perpendicular to that plane, is the tangent to the line of conical intersections in triatomic molecules.

Key to the algorithms discussed in this section is that the quantities in eq 8 are readily evaluated using analytic gradient techniques.[16] In our laboratory it is currently possible to efficiently[16] evaluate these quantities using wave functions with $N^{CSF} > 10^6$.

For $\mathbf{R}_x(2.6) \equiv (R = 2.522, r = 2.6, \gamma = 90°)$, a point on the C_{2v} seam of the conical intersection in AlH_2, Figure 6 reports two nuclear displacement vectors that describe the $g-h(\mathbf{R}_x)$ plane and also displays the corresponding pseudorotation around that conical intersection. Pseudorotation in the $g-h(\mathbf{R}_x)$ plane is expressed in terms of the polar coordinates ρ, a size coordinate, and θ, a "shape" coordinate, defined by $x = \rho \cos\theta$ and $y = \rho \sin\theta$, where $\hat{\mathbf{x}} = \mathbf{h}^{IJ}(\mathbf{R}_x)/||\mathbf{h}^{IJ}(\mathbf{R}_x)||$, $\hat{\mathbf{y}} = \mathbf{g}^{IJ}(\mathbf{R}_x)^\perp/||\mathbf{g}^{IJ}(\mathbf{R}_x)^\perp||$, and $\mathbf{g}^{IJ}(\mathbf{R}_x)^\perp = \mathbf{g}^{IJ}(\mathbf{R}_x) - (\hat{\mathbf{x}}\cdot\mathbf{g}^{IJ}(\mathbf{R}_x))\hat{\mathbf{x}}$.

(b) Locating Points of Conical Intersection. Our algorithm for locating points of conical intersection depends on the observation that starting from a point $\mathbf{R}$ near but not at a conical intersection, a nuclear displacement $\delta\mathbf{R}$ toward the conical intersection at $\mathbf{R}_x = \mathbf{R} + \delta\mathbf{R}$ must satisfy two conditions:[33]

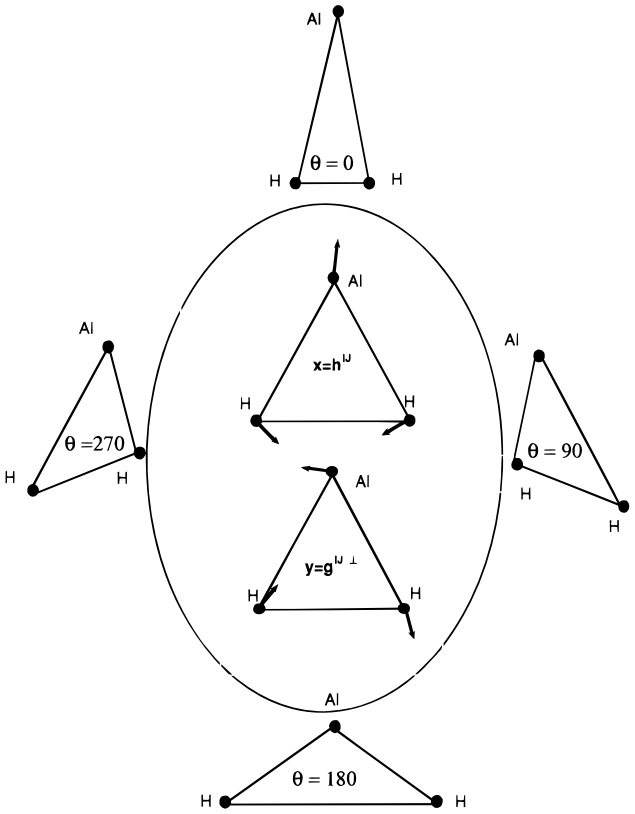

FIGURE 6. $\mathbf{h}^{IJ}(\mathbf{R}_x)/||\mathbf{h}^{IJ}(\mathbf{R}_x)||$ and $\mathbf{g}^{IJ}(\mathbf{R}_x)^\perp/||\mathbf{g}^{IJ}(\mathbf{R}_x)^\perp||$, where $\mathbf{g}^{IJ}(\mathbf{R}_x)^\perp = \mathbf{g}^{IJ}(\mathbf{R}_x) - (\hat{\mathbf{x}}\cdot\mathbf{g}^{IJ}(\mathbf{R}_x))\hat{\mathbf{x}}$ and pseudorotation path in this plane for AlH_2 at $\mathbf{R}_x(r = 2.6a_0)$; see ref 15.

$$E_I(\mathbf{R}) - E_J(\mathbf{R}) + 2\mathbf{g}^{IJ}(\mathbf{R})^\dagger\cdot\delta\mathbf{R} = 0 \tag{9a}$$

$$\mathbf{h}^{IJ}(\mathbf{R})^\dagger\cdot\delta\mathbf{R} = 0 \tag{9b}$$

where eq 9a achieves degeneracy while eq 9b ensures that the wave functions remain eigenfunctions of eq 7. For an intersection to be conical, both $\mathbf{g}^{IJ}(\mathbf{R}_x)$ and $\mathbf{h}^{IJ}(\mathbf{R}_x)$ must be nonvanishing. A complete discussion of the resulting algorithm can be found in ref 16.

Equation 9b has interesting consequences in triatomic molecules where all τ are totally symmetric—a' symmetry. In this case the accidental symmetry-allowed $^{2S+1}A'-{}^{2S+1}A''$ intersection cannot be conical. This should be contrasted with the situation for C_{2v} geometries where the accidental symmetry-allowed $^{2S+1}A_1-{}^{2S+1}B_2$ and $^{2S+1}A_2-{}^{2S+1}B_1$ intersections are conical since a nontotally symmetric mode of b_2 symmetry exists to couple the degenerate states.

(c) Locating Doubly Diabolical Points. The existence of symmetry-allowed conical intersections is comparatively easy to anticipate. In AlH_2, for example, one would restrict the molecule to C_{2v} symmetry ($\gamma = 90°$), fix r, and vary R until $E^2{}_{A_1} = E^2{}_{B_2}$. The process is then repeated with different values of r mapping out the C_{2v} seam of intersection (Figure 7). The additional same-symmetry seam

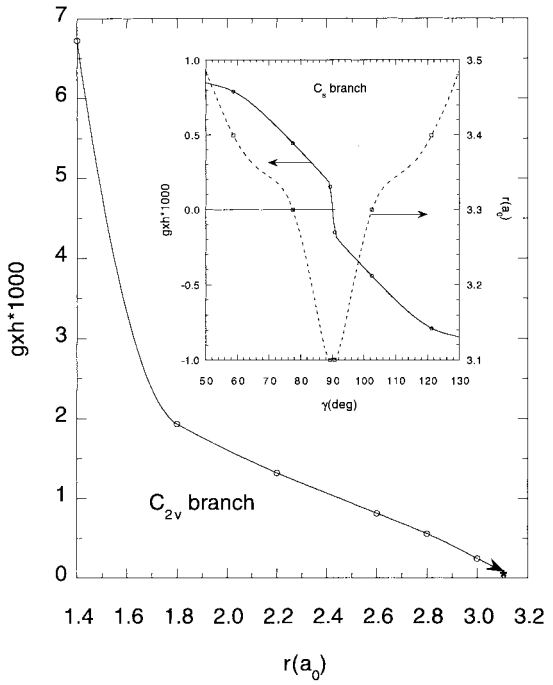

FIGURE 7. For AlH_2 $|\mathbf{g} \times \mathbf{h}|$ as a function of the seam parameter r on the C_{2v} seam. Extrapolation to $\mathbf{g} \times \mathbf{h} = \mathbf{0}$ indicated. Inset: $|\mathbf{g} \times \mathbf{h}|$ and r for the C_s seam as a function of γ. Sign of $\mathbf{g} \times \mathbf{h}$ as in section IIe.

noted above would seem virtually impossible to anticipate. This, however, is not the case. Since $\mathbf{t}^{IJ}$ must vanish at a doubly diabolical point but does not vanish at "standard" conical intersection points, plotting $\mathbf{t}^{IJ}$ along the symmetry-allowed seam reveals the (possible[11]) existence of the same-symmetry seam.

Figure 6 reports $|\mathbf{t}^{IJ}|$ as a function of r and of γ along the C_{2v} and C_s $1^2A' - 2^2A'$ seams of conical intersection in AlH_2. There it is seen that by monitoring $\mathbf{t}^{IJ}$ along the C_{2v} seam of conical intersection, the existence of an intersecting C_s seam can be anticipated. The inset to Figure 6 confirms the vanishing of $\mathbf{t}^{IJ}$ as the doubly diabolical point is approached along the C_s seam. The example in section IIe shows that the C_s seam could exist *in the absence* of the C_{2v} seam, although in that case $\mathbf{t}^{IJ}$ would not vanish at the C_{2v} point on this seam.

(d) Near a Conical Intersection. Using the above-noted perturbation theory, the energies and derivative couplings near $\mathbf{R}_x$ can be expressed in terms of the characteristic parameters[32] $\mathbf{g}^{IJ}(\mathbf{R}_x)$, $\mathbf{h}^{IJ}(\mathbf{R}_x)$, and $\mathbf{s}^{IJ}(\mathbf{R}_x) \equiv (\mathbf{g}^J(\mathbf{R}_x) + \mathbf{g}^I(\mathbf{R}_x))/2$. This analysis will lead to the locally diabatic basis noted in the Introduction and is key to reliable representation of the potential energy, and derivative coupling, surfaces in a form tractable for nuclear dynamics calculations. The existence of a seam of conical intersection considerably complicates representation of the ab initio electronic structure data. In the past this problem has been avoided by "fitting", to the extent possible, the ab initio data with approximate, for example, diatomics in molecules, models. However this approach has inherent limitations. Instead at each $\mathbf{R}_x$ the characteristic parameters can be used to subtract out the "conical part" of the potential energy surface and the singular part of the derivative coupling. The remainder of the potential energy, and derivative coupling, surfaces should be readily described using modern fitting techniques. Below we illustrate these ideas.

Near $\mathbf{R}_x$ it is convenient to use the generalized cylindrical polar coordinates ρ, θ, and $\mathbf{z}$, where ρ, θ were defined above and the unit vectors $\hat{\mathbf{z}}^i$ span the space of dimension $N^{\text{int}} - 2$ orthogonal to the $g-h(\mathbf{R}_x)$ plane.

(i) Energies. In this coordinate system through first order in displacements ($\delta\mathbf{R}$) from $\mathbf{R}_x$

$$E_\pm(\mathbf{R}) = E_I(\mathbf{R}_x) + E_\pm^{(p1)}(\mathbf{R}) \equiv E_I(\mathbf{R}_x) + \mathbf{s}^{IJ}(\mathbf{R}_x)^\dagger \cdot \delta\mathbf{R} \pm \rho q(\theta) \tag{10}$$

where $-$ corresponds to I and $+$ corresponds to J

$$q(\theta)^2 = h_x^2 \cos^2\theta + (g_x \cos\theta + g_y \sin\theta)^2 \equiv h^2 \cos^2\theta + g^2 \sin^2(\theta + \beta) \tag{11a}$$

$$\cos\lambda(\theta) = [h/q(\theta)]\cos\theta \qquad \sin\lambda(\theta) = [g/q(\theta)]\sin(\theta + \beta) \tag{11b}$$

$l_w = \mathbf{l}^{IJ}(\mathbf{R}_x)\cdot\hat{\mathbf{w}}$ for $w = x, y, \mathbf{z}$ and $\mathbf{l}^{IJ} = \mathbf{g}^{IJ}, \mathbf{h}^{IJ}, \mathbf{s}^{IJ}$. From eqs 10 and 11 we have the important result that the $g-h(\mathbf{R}_x)$ plane is privileged in that it contains *all* of the linear part of the energy difference, $E_+(\mathbf{R}) - E_-(\mathbf{R})$.

Figure 8a illustrates the utility of eq 10 reporting, for AlH_2, the energies along circles with $\rho = 0.05a_0$ surrounding $\mathbf{R}_x(2.6)$. The agreement between the computed $E_{1^2A'}$ (that is based on ab initio configuration interaction wave functions) and the prediction of eq 10 (based on those wave functions *at* $\mathbf{R}_x$) is quite good, enabling the conical part of the energy to be treated analytically.

(ii) Derivative Couplings and Diabatic States. Near $\mathbf{R}_x$, $\mathbf{f}^{IJ}(\mathbf{R})$ is given by

$$f_\theta^{IJ}(\mathbf{R}) \cong \left[\frac{1}{2}\frac{\mathrm{d}}{\mathrm{d}\theta}\lambda(\theta)\right] + \left[\rho\frac{\mathrm{d}}{\mathrm{d}\theta}\left(\frac{m_\rho(\theta)}{q(\theta)}\right) + z\frac{\mathrm{d}}{\mathrm{d}\theta}\left(\frac{m_z(\theta)}{q(\theta)}\right)\right] \tag{12a}$$

$$\equiv f_\theta^{(p1),JI}(\mathbf{R}) + f_\theta^{(p2),JI}(\mathbf{R}) \equiv f_\theta^{(p),JI}(\mathbf{R})$$

$$f_\rho^{JI}(\mathbf{R}) \cong m_\rho(\theta)/q(\theta) \equiv f_\rho^{(p),JI}(\mathbf{R}) \tag{12b}$$

$$f_z^{JI}(\mathbf{R}) = m_z(\theta)/q(\theta) \equiv f_z^{(p),JI}(\mathbf{R}) \tag{12c}$$

where

$$\frac{\mathrm{d}\lambda}{\mathrm{d}\theta} = \frac{1}{2}\frac{gh\sin(\beta + \pi/2)}{q^2(\theta)} \tag{13}$$

$$m_w(\theta) = \sum_{i=1}^{K_w}[a_i^w\, p_i^{aw}(\theta) + b_i^w\, p_i^{bw}(\theta)] = q(\theta) f_w^{IJ}$$
$$w = z \text{ or } \rho,\ K_z = 2,\ K_\rho = 3 \tag{14}$$

$$p_n^{aw} = \cos^l\theta \sin^k\theta \sin\lambda(\theta)$$
$$p_n^{bw} = \cos^l\theta \sin^k\theta \cos\lambda(\theta) \tag{15}$$

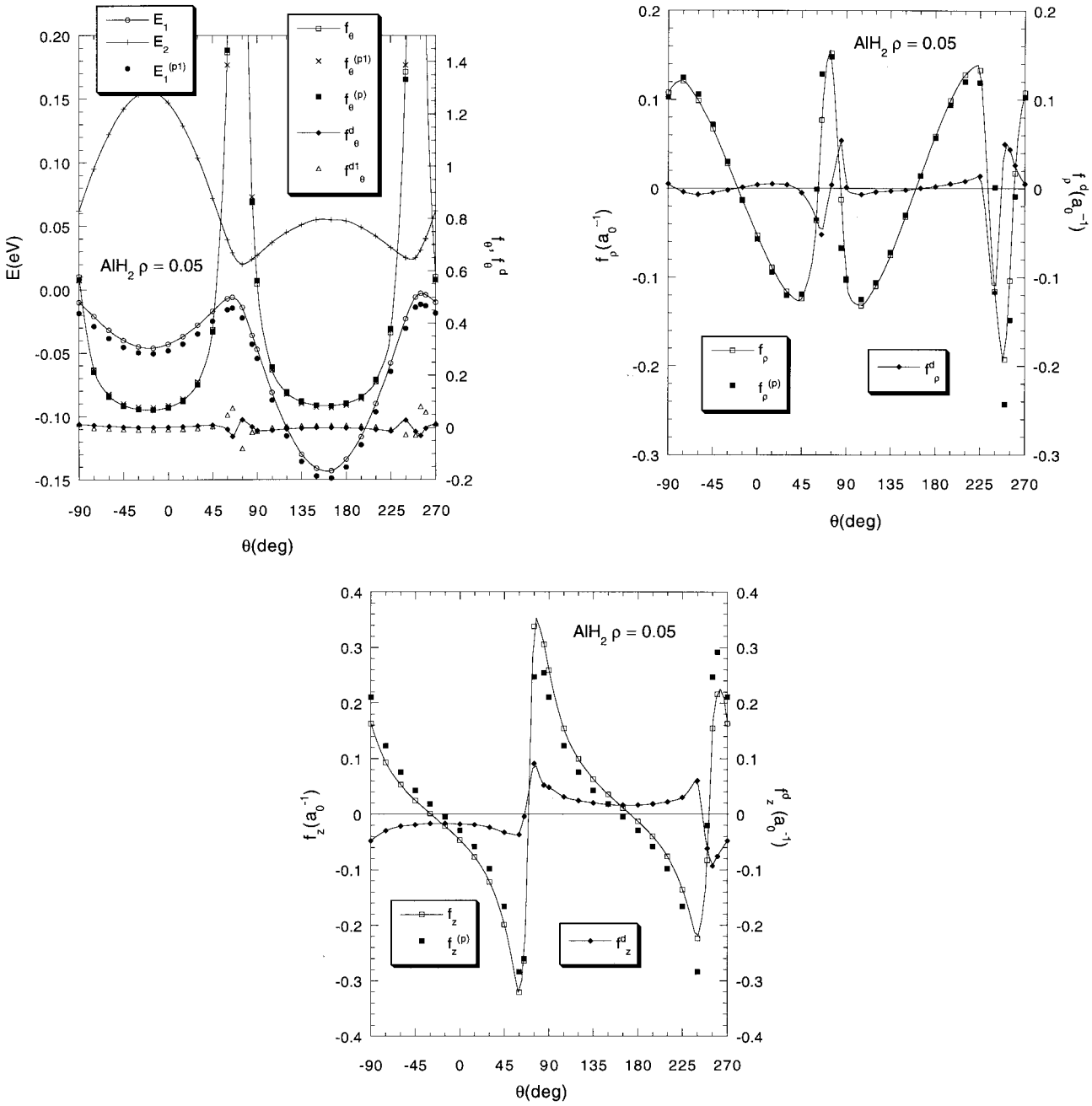

FIGURE 8. (a) For circles in the $g-h$ plane centered at $\mathbf{R}_x(r = 2.6a_0)$ with $\rho = 0.05$: $E_1 \equiv E_{1^2A'}(\mathbf{R})$ (open circles), $E_2 \equiv E_{2^2A'}(\mathbf{R})$ (pluses), $E_1^{(p1)} \equiv E_{1^2A'}^{(p1)}(\mathbf{R})$ (filled circles). Energies in electronvolt relative to $E_{1^2A'}$ at Al (^{2}P) + H_2 asymptote. $f_\theta(\mathbf{R})$ (open squares), $f_\theta^{(p_1)}(\mathbf{R})$ (crosses), $f_\theta^{(p)}(\mathbf{R})$ (filled squares), f_θ^{d} (filled diamonds), and $f_\theta^{\mathrm{d1}} = f_\theta(\mathbf{R}) - f_\theta^{(p1)}(\mathbf{R})$ (open triangles). *IJ* superscript suppressed. (b, c) For circles in $g-h$ plane centered at $\mathbf{R}_x(r = 2.6a_0)$ with $\rho = 0.05$: $f_w(\mathbf{R})$ (open squares), $f_w^{(p)}(\mathbf{R})$ (filled squares), and f_w^{d} (filled diamonds) with (b) $w = \rho$, (c) $w = z$.

and $(w,n,l,k) = (z,1,1,0)$, $(z,2,0,1)$ and $(\rho,1,2,0)$, $(\rho,2,0,2)$, $(\rho,3,1,1)$. As discussed in the following two paragraphs, these equations have important consequences.

From eq 12, at $\mathbf{R}_x$ only $(1/\rho)f_\theta^{IJ}$ is singular, so that the singular part of the derivative coupling can be treated analytically. This result again reflects the privileged nature of the $g-h$ plane. If a different plane had been used to define ρ and θ, f_z^{IJ} would not be small (see below). Equation 14 enables compact expressions for the non-singular components of the derivative coupling at $\mathbf{R}_x$ to be obtained by fitting f_w^{IJ} along a small loop surrounding that point.

The angle $\alpha(\rho,\theta) = \lambda(\theta)/2 + \rho m_\rho(\theta)/q(\theta) + z m_z(\theta)/q(\theta)$ provides the transformation to a pair of approximate diabatic states, $\Psi_I^{\mathrm{d}}(\mathbf{r};\mathbf{R})$,

$$\begin{pmatrix}\Psi_I^{\mathrm{d}}(\mathbf{r};\mathbf{R})\\ \Psi_J^{\mathrm{d}}(\mathbf{r};\mathbf{R})\end{pmatrix} = \begin{pmatrix}\cos\alpha(\rho,\theta) & -\sin\alpha(\rho,\theta)\\ \sin\alpha(\rho,\theta) & \cos\alpha(\rho,\theta)\end{pmatrix}\begin{pmatrix}\Psi_I(\mathbf{r};\mathbf{R})\\ \Psi_J(\mathbf{r};\mathbf{R})\end{pmatrix} \qquad (16)$$

that is, states for which the diabatic derivative coupling

$$f_\tau^{\mathrm{d},IJ} = f_\tau^{IJ} - \frac{\partial \alpha}{\partial \tau} = f_\tau^{IJ} - f_\tau^{(p),IJ} \tag{17}$$

is negligible near the conical intersection (for $\mathbf{R}$ in the $g-h$ plane).[34]

Parts a−c of Figure 8 illustrate these points, reporting for $\mathbf{R}_x(2.6)$ in AlH_2, $f_\tau^{IJ}(\mathbf{R})$, $f_\tau^{(p),JI}(\mathbf{R})$, and $f_\tau^{\mathrm{d},IJ}$ for $\rho = 0.05$, and $\tau = \theta$, ρ, z, respectively. Notice that $(1/\rho)\, f_\theta^{JI}(\mathbf{R}) \gg f_\rho^{JI}(\mathbf{R})$, $f_z^{JI}(\mathbf{R})$ and that $f_\tau^{\mathrm{d},JI}(\mathbf{R})$ is small. Thus, eq 16 in fact defines a viable locally diabatic basis. Observe too that although $f_\theta^{(p1),JI}(\mathbf{R})$ is in good agreement with $f_\theta^{JI}(\mathbf{R})$ inclusion of contributions from $f_\theta^{(p2),JI}$, which reflect information gleaned from $f_\rho^{JI}(\mathbf{R})$, improves the agreement between $f_\theta^{(p),JI}$ and $f_\theta^{JI}(\mathbf{R})$, supporting the validity of the perturbation theory.

IV. Summary and Conclusions

This account discusses recent advances in our understanding of conical intersections. Of particular interest is the role of same-symmetry conical intersections, a class of conical intersections of emerging importance. The existence of same-symmetry conical intersections was once a matter of considerable debate. However, as a result of algorithms that locate conical intersections without prior determination of the potential energy surfaces in question, the existence and importance of this class of conical intersections is now firmly established. Here a new role for this class of conical intersections is emphasized. It is observed that symmetry-allowed conical intersections, intersections readily anticipated owing to the role played by point group symmmetry, need not be isolated features. Rather symmetry-allowed and same-symmetry conical intersections can coexist in the same region of nuclear coordinate space and can in fact intersect. A procedure to anticipate these "doubly diabolical points" based only on the knowledge of the symmetry-allowed intersection is reviewed. Doubly diabolical points are potentially quite important. Their existence means that a symmetry-allowed seam of conical intersection may not provide the complete description of nonadiabatic effects in a particular region of nuclear coordinate space. Determining their prevalence in triatomic and general polyatomic molecules will be an important area of future research.

Also discussed in this work is a perturbative description of the wave functions near a conical intersection. This analysis provides a transformation to a locally diabatic basis and should facilitate representation of the ab initio potential energy, and derivative couplings, surfaces that exhibit conical intersections.

The preparation of this work and the calculations reported herein were made possible by funds provided by the Air Force Office of Scientific Research, the Department of Energy, and the National Science Foundation.

References

(1) *State-Selected and State-to-State Ion−Molecule Reaction Dynamics*, Part 1 and 2; Baer, M., Ng, C.-Y., Eds.; Wiley and Sons: New York, 1991; Vol. 82.
(2) Yarkony, D. R. *Int. Rev. Phys. Chem.* **1992**, *11*, 195−242.
(3) Michl, J.; Bonacic-Koutecky, V. *Electronic aspects of organic photochemistry*; Wiley: New York, 1990.
(4) Hu, X.; Schulten, K. *Phys. Today* **1997**, *50*, 28−34.
(5) Berry, M. V.; Wilkinson, M. *Proc. R. Soc. London, Ser. A* **1984**, *392*, 15−43.
(6) Carrington, T. *Acc. Chem. Res.* **1974**, *7*, 20−25.
(7) Berry, M. V. *Proc. R. Soc. London, Ser. A* **1984**, *392*, 45−57.
(8) *Geometric Phases in Physics*; Shapere, A., Wilczek, F., Eds.; World Scientific: Singapore, 1989.
(9) Mead, C. A. *Rev. Mod. Phys.* **1992**, *64*, 51−85.
(10) Yarkony, D. R. *Rev. Mod. Phys.* **1996**, *68*, 985−1013.
(11) Yarkony, D. R. *Theor. Chem. Acc.* **1997**, *98*, 197−201.
(12) Lengsfield, B. H.; Yarkony, D. R. Nonadiabatic Interactions Between Potential Energy Surfaces: Theory and Applications. In *State-Selected and State to State Ion−Molecule Reaction Dynamics: Theory* (Part 2); Baer, M., Ng, C.-Y., Eds.; Wiley: New York, 1992; Vol. 82, pp 1−71.
(13) Sidis, V. Diabatic Potential Energy Surfaces for Charge-Transfer Processes. In *State-Selected and State-to-State Ion−Molecule Reaction Dynamics: Theory* (Part 2); Baer, M., Ng, C.-Y., Eds.; Wiley and Sons: New York, 1992; Vol. 82, pp 73−134.
(14) Mead, C. A.; Truhlar, D. G. *J. Chem. Phys.* **1982**, *77*, 6090−6098.
(15) Chaban, G.; Gordon, M. S.; Yarkony, D. R. *J. Phys. Chem. A* **1997**, *101*, 7953−7959.
(16) Yarkony, D. R. Electronic Structure Aspects of Nonadiabatic Processes in Polyatomic Systems. In *Modern Electronic Structure Theory*; Yarkony, D. R., Ed.; World Scientific: Singapore, 1995; pp 642−721.
(17) Radazos, I. N.; Robb, M. A.; Bernardi, M. A.; Olivucci, M. *Chem. Phys. Lett.* **1992**, *197*, 217−223.
(18) Matsunaga, N.; Yarkony, D. R. *J. Chem. Phys.* **1997**, *107*, 7825−7838.
(19) Heumann, B.; Duren, R.; Schinke, R. *Chem. Phys. Lett.*, **1991**, *180*, 583.
(20) Carrington, T. *Faraday Discuss. Chem. Soc.* **1972**, *53*, 27−34.
(21) von Neumann, J.; Wigner, E. *Phys. Z.* **1929**, *30*, 467−470.
(22) Teller, E. *J. Phys. Chem.* **1937**, *41*, 109−116.
(23) Mead, C. A.; Truhlar, D. G. *J. Chem. Phys.* **1986**, *84*, 1055.
(24) Mead, C. A. *J. Chem. Phys.* **1979**, *70*, 2276.
(25) Longuet-Higgins, H. C. *Proc. R. Soc. London, A* **1975**, *344*, 147−156.
(26) Yarkony, D. R. *J. Chem. Phys.* **1996**, *104*, 7866.
(27) Keating, S. P.; Mead, C. A. *J. Chem. Phys.* **1985**, *82*, 5102−5117.
(28) Waschewsky, G. C. G.; Kash, P. W.; Myers, T. L.; Kitchen, D. C.; Butler, L. J. *J. Chem. Soc., Faraday Trans.* **1994**, *90*, 1581.
(29) Atchity, G. J.; Ruedenberg, K.; Nanayakkara, A. *Theor. Chem. Acc.* **1997**, *96*, 195−204.
(30) Glezakou, V.-A.; Gordon, M. S.; Yarkony, D. R. *J. Chem. Phys.* **1998**, *108*, 5657−5659.
(31) Mead, C. A. *J. Chem. Phys.* **1983**, *78*, 807−814.
(32) Yarkony, D. R. *J. Phys. Chem. A* **1997**, *101*, 4263−4270.
(33) Manaa, M. R.; Yarkony, D. R. *J. Am. Chem. Soc.* **1994**, *116*, 11444−11488.
(34) Matsunaga, N.; Yarkony, D. R. *Mol. Phys.* **1998**, *93*, 79−84.

AR970113W